Cold breakup of spectator residues in nucleus-nucleus collisions at high energy

J. Aichelin,* J. Hüfner, and R. Ibarra†
Institut für Theoretische Physik der Universität Heidelberg, D-6900 Heidelberg, Federal Republic of Germany and Max-Planck-Institut für Kernphysik, D-6900 Heidelberg, Federal Republic of Germany
(Received 9 November 1983)

Inclusive data from fragmentation reactions of the type $A_P + A_T \rightarrow Z + X$ are analyzed and a reaction mechanism is proposed. A projectile A_P (p, He, α, or Ne) collides with a target nucleus A_T (Au) and one fragment with charge Z and energy E is observed at a solid angle Ω. Projectile energies vary between $84A$ MeV and several A GeV. We propose a parametrization for the triple differential cross section $d^3\sigma/d\Omega\, dE\, dZ$ with six free parameters. The parametrization generalizes the two-vector model which is often used to describe spallation products in proton-nucleus collisions. By fitting data from various experiments we establish a systematics of the six parameters. The experimental values of the parameters can be quantitatively understood in a model where the target nucleus breaks into several fragments similar to the shattering of glass.

I. INTRODUCTION

A bullet is shot through a ball made of glass; the ball shatters into many pieces. A high-energy projectile is shot through a target nucleus; many little fragment nuclei are observed. Does a nucleus shatter like glass when hit by a high-energy projectile? Or are the fragments formed rather like droplets which condense from a vaporized nucleus? These questions are behind the investigation whose result we present here.

In a high-energy nucleus-nucleus collision the straight line motion of the projectile defines an overlap volume of projectile and target matter. Nucleons in the overlap zone are called participants, nucleons outside are called the spectators. Spectator nucleons belong either to the projectile if they are slow in the projectile rest frame or to the target if they are slow in the laboratory frame. This paper deals with medium mass fragments which are believed to originate when the spectator matter of the target breaks up. The geometrical division into participants and spectators is verified experimentally by studying the participants, i.e., the fast nucleons, deuterons, and pions.[1,2] Their distribution in angle and energy indicates that the participant nucleons have come close to thermal equilibrium, therefore the name "fireball."

One distinguishes peripheral reactions and central ones. In a peripheral reaction the overlap between projectile and target nuclei is small and one observes few participants. The spectator pieces are large, i.e., close in mass to the projectile or target nuclei, respectively, and little excited. They decay by evaporating nucleons or light nuclei and/or by fission. The peripheral collisions seem well understood within the abrasion-ablation model.[3,4] A near central collision between two nuclei is characterized by a high multiplicity of participant charges. In coincidence one observes several slow fragments, whose masses A are much smaller than A_T, the mass of the target; typically $4 < A < A_T/3$. We concentrate here on these medium mass fragments. We exclude masses $A \leq 4$ since they may have various origins, e.g., they may be fireball particles or evaporation products. Fission becomes a competing process for $A > A_T/3$. The process which leads to fragment masses in this region has been called "deep spallation," a term which has never received a proper definition in terms of a physical process. Deep spallation processes have been extensively studied in proton-nucleus collisions at high energies. We recall the main properties:

(a) All particle stable nuclei are produced. The mass yield curve $d\sigma/dA$ decreases rapidly with increasing mass until $A \approx A_T/3$. The isotopic distribution $d\sigma/dN$ for Z fixed peaks around the most stable isotope.

(b) The angular distribution $d\sigma/d\Omega$ is essentially isotropic in a system which moves forward with a velocity $v_{\text{c.m.}}$ which is of the order of 1% of the speed of light.

(c) The energy distribution $d\sigma/dE$ in the moving system decays exponentially $\sim \exp(-E/E_0)$ for energies well above the Coulomb barrier. The slope parameter has a value $E_0 \approx 12$ MeV and is practically independent of the reaction and the observed fragment. For small energies, $d\sigma/dE$ shows the effect of Coulomb repulsion. However, $d\sigma/dE$ cannot be fitted by assuming a single Coulomb barrier. A distribution of barriers is required, whose average value is about one half of the one expected from two touching spheres.

The properties of fragments in nucleus-nucleus collisions[5,6] show several similarities to those of proton-nucleus reactions but also some significant differences. For instance, no moving system can be found in which $d\sigma^3/d\Omega\, dE\, dZ$ is isotropic.

None of the above features [(a)—(c)] has yet received a unique and satisfactory explanation. The theoretical approaches may be divided into two classes, those of thermal equilibrium and those of cold, nonequilibrium breakup. In the first class of models,[7-11] the spectator matter receives considerable energy from the reaction and comes to thermal equilibrium. The calculations usually start by assuming an equilibrized hot system with the temperature as a fit parameter. Gross *et al.*[8] find $T = 5.15$ MeV. Then the system decays directly into small particle stable fragments according to the laws of thermo-

dynamics. In most cases the slope of the mass yield curve $d\sigma/dA$ is successfully reproduced. A simultaneous description of the energy and angle dependence $d\sigma^2/d\Omega\, dE$ is not attempted (except by Friedmann *et al.*[10] who assume conventional sequential compound decay). The physical significance of the slope parameter E_0 is unclear in all these approaches. The velocity $v_{\text{c.m.}}$ is never calculated. In the nonequilibrium approaches[12,13] the spectator matter remains essentially cold. The observed fragments are formed because the instability around the fireball zone expands and cracks the spectator matter into pieces. The slope parameter E_0 is then related to Fermi motion[13] or to the temperature of the nucleons around the fireball zone.[12]

What is the correct physics? In order to solve this problem, we proceed in two ways:

(a) We carefully analyze the data of triple differential cross sections and study their variation with projectile mass and projectile energy.

(b) We give a quantitative and comprehensive physical picture of the fragmentation process. We do not claim that our model is the only explanation, but at present it is the only one which describes all the data, i.e., $d\sigma^3/d\Omega\, dE\, dZ$ and not just one aspect of them like $d\sigma/dA$.

New and rather extensive results of triple differential cross sections $d\sigma^3/d\Omega\, dE\, dZ$ for proton-nucleus and nucleus-nucleus collisions

$$A_P + A_T \rightarrow Z + X$$

are published now and form the basis of our investigation.[5,6] In order to analyze them we propose a parametrization of $d\sigma^3/d\Omega\, dE\, dZ$, where six parameters can be adjusted. The parametrization follows from an intuitive picture for the reaction but seems sufficiently general to describe all the data (Sec. II). The experimental data are well fitted by the parametrization of $d\sigma^2/d\Omega\, dE$. The physics of the data (variation with energy and projectile) is then fully contained in the six parameters and their systematics (Sec. III). The mathematical formalism behind the parametrization is presented in Secs. IV and V, where microscopic expressions are derived for all six parameters. Section VI is devoted to the comparison between calculated parameters and those from the fit to the data. We close with a summary and conclusions (Sec. VII).

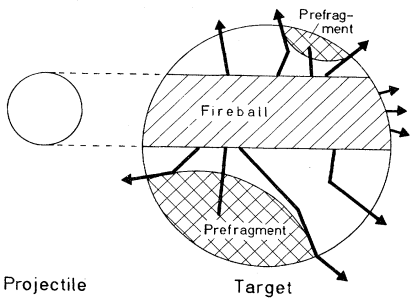

FIG. 1. Our intuitive picture: A projectile hits the target. The overlapping zones of target and projectile form a fireball. Fireball nucleons (black streaks) enter the cold spectator matter and deposit energy and momentum. This leads to a global destabilization of the spectator matter and finally to fragmentation.

II. THE MODEL

The model which we propose is based on nonequilibrium physics. We view fragmentation as a process similar to the shattering of glass, but one should be cautious and not carry this analogy too far. The intuitive picture of the model is visualized in Fig. 1. Fragmentation is a two-step process. In the first step the participant nucleons form a fireball and the spectator matter remains cold. The fireball is described by three quantities: the number of participants, their temperature, and their average momentum in the beam direction. In the second step the fireball decays. Some participants escape without any further collision, mostly at forward angles. Other participants enter into the spectator matter and deposit energy and momentum. Locally, bonds are weakened and the spectator matter is destabilized globally and cracks. The participants which have penetrated the spectator matter can either escape or are captured. If captured, the deposited energy and momentum help to "break off" a piece of matter in already globally destabilized nuclear matter. The Coulomb force also pushes the pieces apart. They are called prefragments. They are usually excited and evaporate a few nucleons before they are observed as fragments.

This physics is contained in the following parametrization of the triple differential cross section:

$$\frac{d\sigma^3}{dE\, d\Omega\, dZ} = \frac{d\sigma}{dZ}(Z,s,\sigma_F) \int_0^{V_C^{\max}} dV_C g(V_C) f(E,\Omega,v_{\text{c.m.}},p_{||},\Delta,V_C) , \tag{2.1}$$

which we explain in this section. Detailed derivations are relegated to Secs. IV and V. In Eq. (2.1) Z is the charge of the observed fragment, with E its kinetic energy, and Ω the solid angle, both in the laboratory frame. The variables E and Ω can also be converted to a momentum $\vec{p}$. The total fragmentation cross section is denoted by σ_F and the dimensionless parameter s describes the shape of the charge yield curve. Before breakup the target spectator matter moves with velocity $v_{\text{c.m.}}$ in the laboratory. In the rest system of the target spectator the fragment has a momentum distribution characterized by a width Δ and a mean momentum $p_{||}$ in the beam direction. V_C denotes the Coulomb barrier between the prefragment and the remainder.

The final momentum $\vec{p}$ of the prefragment is a sum of four different contributions:

(a) In the rest frame of the target spectator the separated prefragment has a momentum $\vec{p}_1$ which is isotropically distributed and most probably arises from Fermi motion.

(b) The decaying fireball imparts a momentum $\vec{p}_2$ to each prefragment. The distribution of $\vec{p}_2$ in the target spectator rest frame has a mean momentum $p_{||}$ in the direction of the beam and a width related to the temperature T of the fireball.

(c) When rolling down the Coulomb barrier the prefragment gains energy and therefore momentum,

$$E_{\text{final}} = V_C + \frac{(\vec{p}_1+\vec{p}_2)^2}{2M} , \tag{2.2}$$

where M is the mass of the prefragment and V_C the Coulomb energy.

(d) Due to the "viscosity," the process of fireball formation transfers momentum to the target spectator piece before decay. This results in a mean forward velocity $\vec{v}_{\text{c.m.}}$ of all fragments in the laboratory frame.

For $p_{||}=0$, i.e., isotropic decay in the moving system, our momentum distribution is the same as in the two vector model for proton-nucleus collisions.[14] However, the data from nucleus-nucleus collisions cannot be fitted with $p_{||}=0$. We assume Gaussian functions for the distributions of $\vec{p}_1$ and $\vec{p}_2$. Their folding leads to the following form of the energy distribution in the laboratory system:

$$f(E,\Omega,v_{\text{c.m.}},p_{||},\Delta,V_C) = c \left\{ \exp - \frac{\left[\left[1-\frac{2MV_C}{(\vec{p}-\vec{p}_{\text{c.m.}})^2} \right]^{1/2} (\vec{p}-\vec{p}_{\text{c.m.}}) - \vec{p}_{||} \right]^2}{\Delta} \right\}$$
$$\times V_p \left[1-\frac{2MV_C}{(\vec{p}-\vec{p}_{\text{c.m.}})^2} \right]^{1/2} \theta[(\vec{p}-\vec{p}_{\text{c.m.}})^2 - 2MV_C] , \tag{2.3}$$

where $\vec{p}_{\text{c.m.}} = M\vec{v}_{\text{c.m.}}$. The last factor is the Jacobian for the transformation from the center of mass to the laboratory system. The distribution is normalized to 1:

$$\int f(E,\Omega,v_{\text{c.m.}},p_{||}\Delta,V_C)dE\, d\Omega = 1 . \tag{2.4}$$

Expression (2.3) is the energy and angle distribution for a given value V_C of the Coulomb barrier. The data cannot be fitted by this expression, even if the value of V_C is adjusted. Rather, the data require a distribution of Coulomb barriers $g(V_C)$. This has been realized also in p-A collisions.[15] In our picture the distribution $g(V_C)$ arises from the fact that the prefragments originate from different sites in the target. Depending on the place where they are produced they gain different kinetic energy due to the Coulomb field. This picture results in the following distribution:

$$g(V_C) = \frac{3}{2} \frac{\sqrt{V_C}}{(V_C^{\max})^{3/2}} \theta(V_C^{\max} - V_C) , \tag{2.5}$$

where $V_C^{\max}$ is the maximum Coulomb energy the prefragment can gain by the remainder and should correspond to prefragments originally situated at the target surface.

The charge yield curve $d\sigma/dz$ reflects the distribution of "cracks" in the spectator matter. We do not know the detailed mechanism for how the cracks form. Therefore we approach the problem by the principle of minimum information (cf. also Aichelin *et al.*[16]). We *assume* all possible fragmentations of the target spectator (which contains Z_0 charges) to be equally probable. This is a minimal assumption. If the consequences agree with experiment as we shall show, no further information is contained in the data. Our assumption has the same character as the fundamental assumptions of statistical mechanics. At the moment, we are unable to justify the assumption. From this assumption we derive in Sec. IV the shape of $d\sigma/dZ$ to be

$$\frac{d\sigma}{dZ} = \sigma_F \frac{1}{e^{Z\cdot s}-1} . \tag{2.6}$$

Here, σ_F is the integrated cross section for multifragmentation of the target and the second factor represents the mean multiplicity of fragment Z, and contains one parameter s.

We use Eq. (2.1) to fit the experimental data. It allows us to condense the many data points which constitute the experimental triple differential cross section into a set of six parameters. They depend on the beam energy E_P (for $p_{||}$, Δ, $v_{\text{c.m.}}$, σ_F, and s), the projectile mass A_P (for $v_{\text{c.m.}}$, σ_F, s, and $V_C^{\max}$), and on the prefragment charge Z (for Δ, and $V_C^{\max}$).

III. FITTING PROCEDURE

We apply a χ^2 fit routine to analyze the available data and to determine the free parameters of Eq. (2.1). Triple differential cross sections by Warwick *et al.*[5] and Bock *et al.*[6] are analyzed. In the experiment from the Bevalac[5] a gold target is used and the projectiles are p, He, and Ne at energies from 250A MeV to several A GeV. The second class of experiments[6] uses the beam of 84A MeV from the synchrocyclotron at CERN with oxygen projectiles and gold as the target.

As mentioned above, the prefragments have some excitation energy due to the absorption of energy from the fireball nucleons and possibly due to a change of their shape. Hence they will evaporate some nucleons or light fragments before they are observed as fragments. We checked that the influence of the evaporation on the energy distribution $d\sigma^2/d\Omega\, dE$ can be neglected, whereas the influence on $d\sigma/dZ$ cannot and will be discussed below. The cross section (2.1) for a given fragment charge has six parameters to be fitted. The inclusion of each further fragment require two additional parameters because $V_C^{\max}$

and Δ depend on the prefragment charge. Due to limited computer time we fit, at most, eight parameters simultaneously (i.e., data for two fragments). This corresponds to a central processing unit time of one minute on a CRAY-1. A fit of the parameters σ_F and s, which describe the charge distribution, is only meaningful, however, if one can include many different fragments. Since this is not possible we split the fit procedure into two parts: The first part concerns the momentum distribution $d\sigma^2/d\Omega\, dE$ of one fragment and we determine the following five free parameters: Δ, $v_{\text{c.m.}}$, $V_C^{\max}$, $p_{||}$, and $d\sigma/dZ$. Then we determine the distribution $d\sigma/dZ$. In the first run the momentum distribution of each fragment is fitted separately. We check the consistency of our model by fitting two fragments simultaneously under the constraint that $p_{||}$ and $v_{\text{c.m.}}$ are the same for both fragments. In these cases χ^2 per degree of freedom is between those values obtained by fitting each fragment separately.

For each fit of $d\sigma^2/d\Omega\, dE$ we try at least 16 different starting points. All searches reach the same minimum. For one fit we have investigated the steepness of the minimum: The χ^2 per degree of freedom changes by about 2.5% if one changes separately the parameters $d\sigma/dZ$ by 2.8%; Δ by 10%; $p_{||}$ by 15%; $v_{\text{c.m.}}$ by 13%; and $V_C^{\max}$ by 2.6%. If one changes the parameters $p_{||}$, $v_{\text{c.m.}}$, and Δ simultaneously, the change of χ^2 is smaller. We suppose that this is about the same for the other reactions.

Figure 2 shows a comparison between the fit for $d\sigma^2/d\Omega\, dE$ and the data by Warwick[5] for six reactions. The data are well reproduced by the fit. The same holds true for the data of Bock *et al.*[6] for reactions at 84A MeV (Fig. 3). This comparison proves that the parameters which we introduced are sufficent to describe the data; the steepness analysis shows that these parameters are also necessary.

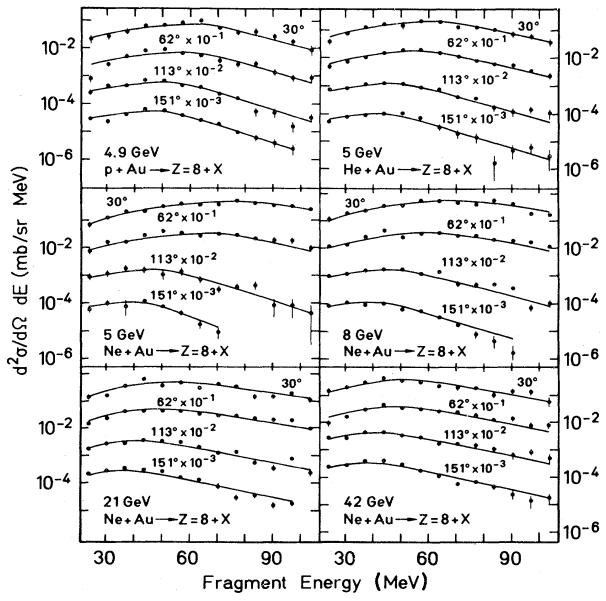

FIG. 2. Experimental and fitted double differential cross sections $d^3\sigma/d\Omega\, dE\, dZ$ of fragments of charge $Z=8$ for the reactions measured by Warwick *et al.* (Ref. 5).

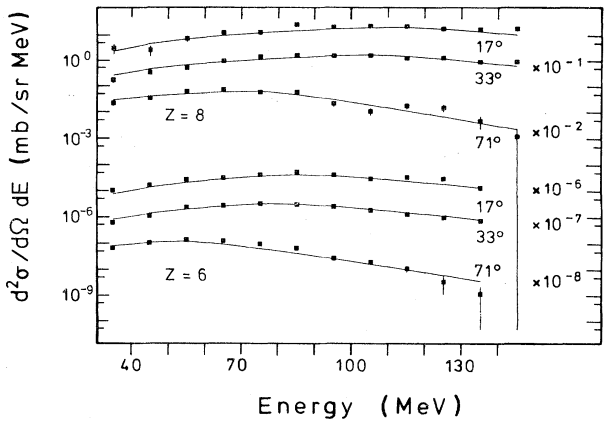

FIG. 3. Experimental and fitted double differential cross sections of $Z=8$ fragments for 84A MeV projectiles ^{16}O (above) and ^{12}C (below) on a gold target. The unit on the ordinate should read μb instead of mb. The experiment is by Bock *et al.* (Ref. 6).

We turn to the shape of the charge yield curve $d\sigma/dZ$ as a function of Z. As shown in Sec. IV, expression (2.6) is derived for the distribution of prefragments. During the evaporation chain the shape of $d\sigma/dZ$ will be changed: There will be an average shift of one or two units of Z to lower Z. Furthermore, due to strong fluctuations in the particle thresholds for different values of Z, the charge yield curve shows strong variations, particularly for low values of Z. Thus the theoretical shape $d\sigma/dZ$ for the prefragments will be only an approximation to the experimental fragment distribution. Therefore, we prefer to compare the data with the theoretical prediction (2.6) where the calculated value of s is used (see Sec. IV), rather than to fit the shape [Eq. (2.6)] to the data. Figure 4 shows a typical result: The solid lines reproduce the data in an average way.

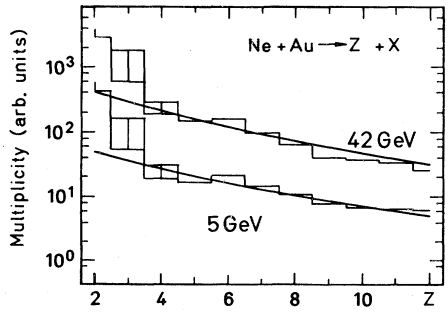

FIG. 4. Experimental and theoretical charge yield curves for fragments created in the reaction Ne + Au$\rightarrow Z + X$ (Ref. 5) for two different beam energies. The shape of the calculated curve (solid line) is completely determined from theory. The theoretical and experimental curves are normalized to each other by requiring the theoretical total yield for $Z>4$ to be the same as the experimental one.

IV. THE CHARGE YIELD CURVE IN MULTIFRAGMENTATION

The target spectator piece of charge Z_0 breaks into several fragments. The detailed macroscopic mechanism is unknown. All authors who treat this problem admit this. They replace the correct treatment by some assumptions. There are various assumptions, yet they have one feature in common: They are based on statistical and/or geometrical arguments. We do the same. Our basic assumption is the following: All possible fragmentations of the spectator charge are equally probable.

What is a "fragmentation?" We define it in terms of partitions. A partition of a number N is a decomposition of N into integers n_i $n_1<n_2<n_3$ which have multiplicities m_1,m_2, etc., irrespective of their order. For example, for $N=3$ exist the following three partitions: (1,1,1), (1,2), and (3). Intuitively we think that the requirement of equal probability for each partition describes fragmentation similar to the shattering of glass. Other definitions of fragmentation are possible and are discussed in the Appendix. We call $A(N)$ the number of all possible distinct partitions of the number N,

$$A(N)=\sum_{\{m_1,m_2,\ldots,m_n\}}\delta\left[N-\sum_{k=0}^{\infty}m_k k\right]. \tag{4.1}$$

Then

$$B(N,n)=\sum_{\{m_1,m_2,\ldots,m_n\}}\delta\left[N-\sum m_k k\right]m_n \tag{4.2}$$

is the number of fragments of charge n which are found in an ensemble of all possible partitions.

The average multiplicity to observe a fragment of charge n is given by

$$W(N,n)=\frac{B(N,n)}{A(N)}. \tag{4.3}$$

The values of $W(N,n)$ can be calculated analytically from the recursion relations

$$\begin{aligned}&B(N,n)=B(N-n,n)+A(N-n),\\&A(N)=\sum_n\frac{nB(N,n)}{N}.\end{aligned} \tag{4.4}$$

In order to have expressions which give $W(N,n)$ in a simple form, we introduce Laplace transforms. In the language of thermodynamics we go from a microcanonical ensemble (where the total number N is prescribed) to a canonical ensemble where we require only the mean value $\langle N\rangle$ to be fixed. We introduce

$$W(s,n)=\frac{B(s,n)}{A(s)}, \tag{4.5}$$

where

$$\begin{aligned}A(s)&=\int_0^\infty dN\exp(-sN)A(N)\\&=\sum_{\{m_1,\ldots,m_n\}}\exp(-s\sum m_k k)\\&=\prod_i\frac{1}{1-\exp(-si)},\end{aligned} \tag{4.6}$$

$$\begin{aligned}B(s,n)&=\int_0^\infty dN\exp(-sN)B(N,n)\\&=\prod_{i\neq n}\frac{1}{1-\exp(-si)}\frac{1}{s}\frac{d}{dn}\frac{1}{1-\exp(-sn)}.\end{aligned}$$

The value of s is fixed by the requirement that

$$N=-\frac{d}{ds}\ln A(s)\Big|_{s=s(N)} \tag{4.7}$$

We find (see the Appendix for details)

$$s(N)=1.28/\sqrt{N}. \tag{4.8}$$

Then, Eq. (4.5) leads to

$$W(N,n)=\frac{1}{\exp(1.28n/\sqrt{N})-1}, \tag{4.9}$$

which is the mean multiplicity for a fragment of charge n if a piece of N charges is decomposed according to the principle of equal partitions. The exact multiplicity $W(N,n)$ [Eqs. (4.3) and (4.4)] and the one calculated using the Laplace transforms [Eq. (4.9)] agree well for $N>35$ and $n>2$.

We return to the fragmentation cross section $d\sigma/dZ$. We postulate that $d\sigma/dZ$ is given by the total fragmentation cross section σ_F times the multiplicity $W(Z_0,Z)$. What is Z_0? We assume that neither the participants nor the projectile spectators contribute to fragmentation. Therefore we have to subtract the fast charges Z_{fast} and define Z_0 by

$$Z_0=Z_P+Z_T-Z_{\text{fast}}, \tag{4.10}$$

where Z_P and Z_T are the charges of projectile and target, respectively, and Z_{fast} are the charges of the observed fast particles (essentially fireball charges). Note that Eq. (4.9) with $N=Z_0$ determines the slope of the charge yield curve completely. As can be seen in Fig. 4, the shape of the experimental distribution $d\sigma/dZ$ is quantitatively reproduced for $Z>3$. Fragments with lower charges may also originate from processes other than fragmentation, and we leave them out. For instance, in a peripheral reaction the target nucleus is excited and evaporates nucleons and light nuclei. They may be responsible for the large increase of the experimental cross sections at $Z<3$.[17] Equation (4.9) can also be derived using the principle of minimal information.[16]

V. CALCULATION OF KINEMATICAL PARAMETERS

A. Energy and angle distribution of the prefragments

If the participant nuleons have reached thermal equilibrium, the momentum distribution of the fireball nucleons is (nonrelativistically)

$$g(\vec{p},b)=\frac{N(b)}{[2\pi mT(b)]^{3/2}}\exp-\frac{[\vec{p}-\vec{p}_{||}(b)]^2}{2mT(b)}. \tag{5.1}$$

Here, the number N, the mean momentum $\vec{p}_{||}$, and the temperature T are functions of the impact parameter b; m is the mass of the nucleon. Assuming that all nucleons

in the geometrical overlap are participants whereas the rest are spectators, $N(b)$, $p_{||}(b)$, and $T(b)$ can be calculated from geometry and the conservation of energy and momentum. $T(b)$ has to be corrected for the production of pions. Some fireball nucleons penetrate the spectator matter, carry their momentum into it, and deposit it into the prefragment. We call $\alpha\cdot\vec{p}$ the fraction of momentum which the prefragment receives from the fireball, where $\vec{p}$ is distributed according to the function $g(\vec{p},b)$. According to our analysis the momentum flow from the fireball to the prefragment is small. The main part of the momentum distribution is isotropic in the target rest frame and arises from Fermi motion: If a prefragment is cut out of a nucleus in a rapid way, it is left with an isotropic momentum distribution whose mean square value is given by Goldhaber.[18]

$$\Delta_F=\langle p^2\rangle=\frac{k_F^2}{5}A\frac{A_T-A}{A_T-1}\ , \tag{5.2}$$

where k_F denotes the Fermi momentum, and A and A_T represent the nucleon numbers of the prefragment and target, respectively.

If we assume a Gaussian distribution for the Fermi momenta, the momentum distribution of the prefragment is obtained by folding this Gaussian and the one of Eq. (5.1), with the result

$$f(\vec{p},b)=C\exp-\frac{[\vec{p}-\alpha\vec{p}_{||}(b)]^2}{\Delta_F+\alpha 2mT}\ . \tag{5.3}$$

We then add the effect of the Coulomb repulsion as described by Eq. (2.2). Then the momentum distribution in the spectator rest frame has the form ($\vec{e}_p=\vec{p}/p$),

$$f(\vec{p},b)=C\exp-\frac{[\sqrt{(p^2-2MV_C)}\vec{e}_p-\alpha\vec{p}_{||}(b)]^2}{\Delta_F+\alpha 2mT(b)}\times\theta(p^2/2M-V_C)\ . \tag{5.4}$$

As long as the projectile dives fully into the target the quantities $N(b)$, $p_{||}(b)$, and $T(b)$ depend little on the impact parameter b. We replace them by average values denoted by $T_{\rm FB}$, $(p_{||})_{\rm FB}$, and $N_{\rm FB}$.

Due to viscosity between the fireball and the whole spectator matter, the spectator matter receives some mean forward velocity $v_{\rm c.m.}$. This is explained below. Here we use $v_{\rm c.m.}$ to transform Eq. (5.4) into the laboratory system, then we integrate over the distribution of Coulomb barriers and obtain Eqs. (2.3) for $d\sigma^2/d\Omega\,dE$. The parameters Δ and $p_{||}$ in Eq. (2.3) can be calculated by

$$\Delta=\Delta_F+2m\alpha T_{\rm FB}\ ,\qquad p_{||}=\alpha(p_{||})_{\rm FB}\ . \tag{5.5}$$

We expect α to be of the order one (one fireball nucleon is absorbed in the prefragment).

By absorbing the fireball nucleons and by forming a spherical surface the prefragment gains excitation energy. This energy is of the order of several MeV per nucleon. The prefragment deexcites by evaporation. We estimate that this process shifts the final energy E of the fragment by about 1 MeV with respect to the prefragment distribution and can therefore be neglected.

B. Distribution of Coulomb barriers

Energy spectra of fragments emitted in high-energy nucleus-nucleus collisions exhibit a broad peak and then an exponential decay (Fig. 2). The peak is usually attributed to the Coulomb repulsion. However, the situation is complicated: If the compound nucleus (projectile plus target) would break up into a fragment and a remainder, the energy distribution of the fragment would show a sharp dropoff for energies $E<V_C^{\rm nom}$, where the "nominal barrier"

$$V_C^{\rm nom}=\frac{ZZ'e^2}{r_0'[A^{1/3}+(A_T+A_P-A)^{1/3}]}\ ,\qquad Z'=Z_T+Z_P-Z \tag{5.6}$$

is the Coulomb energy of two touching spheres ($r_0'\cong 1.4$ fm) which have charges Z and Z', respectively. Since the experimental spectra show a broad peak, there must be a distribution $g(V_C)$ of Coulomb barriers. Satisfactory fits to the experimental p-A data are obtained by assuming a step function $g(V_C)$ with two parameters.[20] The center of $g(V_C)$ is at $V_C=\kappa\ V_C^{\rm nom}$, where $\kappa\approx 0.5$, and the width of $g(V_C)$ is about $0.4\,V_C^{\rm nom}$. No justification is given for the choice of the distribution function, nor for the width and the value of κ.

In this subsection we derive the shape of the distribution function $g(V_C)$ which we utilize to analyze the experimental data. The essential idea is the following: The Coulomb barrier varies because a fragment of charge Z escapes from different locations inside the target spectator matter. However, the distribution of spectator matter depends on time. We assume for it a uniform charge distribution which expands isotropically. Of course, this is an idealization of the true situation, where originally a hole is drilled out of the target nucleus. The Coulomb barrier corresponds to the asymptotic kinetic energy which the fragment receives from the Coulomb force exerted during the expansion phase.

The electrostatic potential energy of a spherical fragment with charge Z *inside* a uniformly charged sphere with charge Z_0-Z is

$$V_C(r)=\frac{3}{2}\frac{(Z_0-Z)Ze^2}{R^3}(R^2-R_F^2/5-r^2/3)\quad(r\le R)\ , \tag{5.7}$$

where R_F and R are the radii of the fragment and of the uniform charge distribution, respectively (Fig. 5). The force $F(r)$, derived from Eq. (5.7), is

$$F(r)=\frac{Z(Z_0-Z)e^2}{R^3}r\quad(r\le R)\ . \tag{5.8}$$

Since the broken up spectator matter expands, not only does the position $r(t)$ of the fragment vary with time but also the global radius $R(t)$. For a uniform and isotropic expansion, $r(t)/R(t)=r(0)/R(0)$. Then the asymptotic

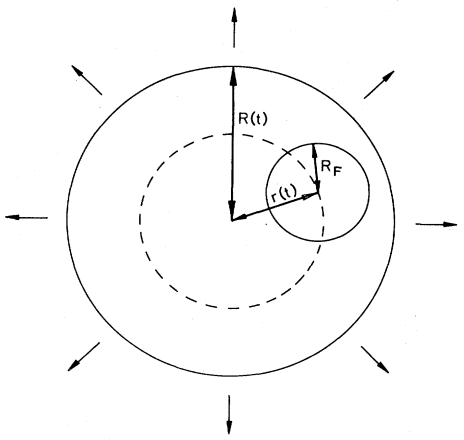

FIG. 5. The Coulomb energy for an isotropically expanding charge distribution of radius $R(t)$. A prefragment of radius R_F is located at a distance $r(t)$ from the center. This fragment only feels the Coulomb force from the charges contained in a sphere with radius $r(t)$.

kinetic energy $(K)_\infty$ of the fragment initially at distance $[r_0 \equiv r(0),\ R_T \equiv R(0)]$ is obtained as

$$(K)_\infty = \int_{r_0}^{\infty} F(r)dR = Z(Z_0-Z)e^2 \int_{r_0}^{\infty} (r/R^2)dr = \frac{Z(Z_0-Z)e^2 r_0^2}{R_T^3} = V_C(r_0) . \quad (5.9)$$

The fragment can originate anywhere from inside the nucleus, i.e., from all radii $r_0 \le R_{\max}$ corresponds to the maximal radius from which the fragment escapes. Therefore the distribution of Coulomb barriers $g(V_C)$ obeys the equation

$$g(V_C)dV_C = r_0^2\, dr_0 , \quad (5.10)$$

from which

$$g(V_C) \propto r_0 \propto \sqrt{V_C} \quad (5.11)$$

for radii $r_0 \le R_{\max}$. Normalized to 1, the distribution function takes the form

$$g(V_C) = \frac{3}{2}\left[\frac{V_C}{(V_C^{\max})^3}\right]^{1/2} \theta(V_C^{\max}-V_C) , \quad (5.12)$$

where the maximal Coulomb barrier $V_C^{\max}$ corresponds to $R_{\max}$, the largest radius from which a prefragment can arise. We take $V_C^{\max}$ as a fit parameter, which is determined from experiment. According to our picture this parameter can be calculated by

$$V_C^{\max} = \left[\frac{R_{\max}}{R_T}\right]^2 \left[\frac{(Z_0-Z)Ze^2}{R_T}\right] , \quad (5.13)$$

where Z_0 is defined by Eq. (4.12) and R_T is the radius of the target nucleus. Then, according to Fig. 5,

$$R_{\max} = R_T - R_F . \quad (5.14)$$

Although our distribution function $g(V_C)$ [Eq. (5.12)] does not have the functional form of a step function, as employed in the analysis of the p-A data, the average properties, mean value, and mean square deviation of our $g(V_C)$ correspond to those previously employed. If we define the reduction factor κ as the ratio of the mean value

$$\langle V_C \rangle = \int_0^{V_C^{\max}} V\, dV\, g(V) \quad (5.15)$$

to a nominal value V_C^{nom} calculated with charges Z_0-Z and Z and a radius R_T+R_F, we find

$$\kappa = \frac{\langle V_C \rangle}{V_C^{\text{nom}}} = \frac{3}{5}\left[\frac{R_{\max}}{R_T}\right]^2 (1+R_F/R_T) , \quad (5.16)$$

and for the width

$$\Delta_C = (\langle V_C^2 \rangle - \langle V_C \rangle^2)^{1/2}/V_C^{\text{nom}} = 0.26\left[\frac{R_{\max}}{R_T}\right]^2 (1+R_F/R_T) . \quad (5.17)$$

Our distribution function has the properties which have been assumed to describe earlier experiments on p-A collisions.[20] The comparison with the data for nucleus-nucleus collisions will be relegated to Sec. VI.

C. Velocity of the target in the laboratory system

In the first step of the fragmentation reaction the projectile penetrates the target and a fireball is formed. The spectator matter remains cold but receives a mean velocity $v_{\text{c.m.}}$ This velocity is observed experimentally but has never been explained quantitatively. We propose the following mechanism: During the formation of the fireball, nucleons which have been bound to the spectator matter become free. In this process the bonds are stretched until they break. During stretching, the spectator matter is accelerated. We cast this picture into formulae (cf. Abul-Magd *et al.*[19]).

A particle of mass m is bound by the energy B. Suddenly it receives momentum $\vec{p}$, the bond is broken, and the particle escapes with momentum $\vec{K}$. Energy conservation leads to

$$\frac{\vec{K}^2}{2m} = \frac{\vec{p}^{\,2}}{2m} - B . \quad (5.18)$$

We assume the vector $\vec{K}$ to have the same direction as $\vec{p}$. This implies that

$$\vec{K} = a\vec{p} , \quad (5.19)$$

where $a < 1$. The difference $\vec{p}-\vec{K}$ has to be taken up by the object to which the nucleon had been bound (in our case in the spectator matter). We call $1-a$ the viscosity coefficient. Equation (5.18) then reads as follows:

$$\frac{p^2}{2m}(1-a^2) = B . \quad (5.20)$$

If the transferred energy $p^2/2m$ is large compared to the binding energy B, which is the case in high-energy reactions, Eq. (5.20) has the solution

TABLE I. The numerical values for the fitted parameters which characterize the energy and angle distribution $d^3\sigma/d\Omega\, dE\, dZ$ in the parametrization given in Sec. II for reactions which lead to $Z=8$ fragments at various projectile energies E. The parameters are of the overall normalization $d\sigma/dZ$, the width Δ and the shift $p_{||}$ of the fragment momentum distribution in the spectator rest system, the velocity $v_{\text{c.m.}}$ of this system with respect to the laboratory, and the maximal Coulomb barrier $V_C^{\max}$ felt by the fragment. The last two columns contain the values $(p_{||})_{\text{FB}}$ and T_{FB} for the fireball. They are calculated under the assumption of complete thermalization among all participants.

Projectile/Target	E (A GeV)	$d\sigma/dZ$ (mb)	Δ (GeV/c)^2	$p_{||}$ (GeV/c)	$v_{\text{c.m.}}$ (c)	$V_C^{\max}$ (MeV)	$(p_{||})_{\text{FB}}$ (GeV/c)	T_{FB} (MeV)
Ne/Au	0.25	160	0.42	0.15	0.019	58.1	0.19	24
Ne/Au	0.4	170	0.45	0.22	0.012	53.8	0.24	31
Ne/Au	1.0	220	0.56	0.07	0.0085	43.5	0.38	58
Ne/Au	2.1	200	0.52	0.001	0.007	42.0	0.50	89
He/Au	1.2	80	0.44	0.07	0.009	50.7	0.30	54
p/Au	4.9	33	0.42	0.06	0.005	53.2	0.50	103
O/Au	0.84	440	0.43	0.28	0.030	64.2	0.10	11

$$(1-a)\approx\frac{B}{p^2/m}\ . \tag{5.21}$$

If the bonds of n particles are broken, the target spectator has an average parallel momentum of

$$\langle p_{||}\rangle = n(1-a)(p_{||}) = n\frac{B}{(\vec{p}^{\,2}/m)}(p_{||})\ . \tag{5.22}$$

We identify the average values of $(p_{||})$ and $(p^2/2m)$ on the right-hand side of Eq. (5.22) with the mean values $(p_{||})_{\text{FB}}$ and $\frac{3}{2}T_{\text{FB}}$ for the fireball. Then the velocity of the target spectator in the laboratory frame is a function of $(p_{||})_{\text{FB}}/T_{\text{FB}}$ and can be calculated by

$$v_{\text{c.m.}} = \frac{1}{3}\frac{n}{A_0}\frac{B}{m}\left[\frac{p_{||}}{T}\right]_{\text{FB}} = \gamma\left[\frac{p_{||}}{T}\right]_{\text{FB}}, \tag{5.23}$$

where A_0 is the mass of the target spectator. We take n to be the number of nucleons from the interface between participant and spectator matter. For $B=16$ MeV and a thickness of the interface of 1 fm, γ is around 0.001. Equation (5.23) is certainly not an exact formula but should reproduce the trend and the order of magnitude of the experimental values.

VI. COMPARISON BETWEEN EXPERIMENT AND CALCULATON

Experimental data for triple differential cross sections have been analyzed using the parametrization [Eq. (2.1)] and the fit procedure explained in Sec. III. We recall the form of the triple differential cross section,

$$\frac{d^3\sigma}{dE\, d\Omega\, dZ} = \frac{d\sigma}{dZ}\int dV_C g(V_C) f(E,\Omega,v_{\text{c.m.}},p_{||},\Delta,V_C)\ . \tag{2.1}$$

Table I contains the numerical values of the fitted parameters for various reactions which we discuss in detail. We begin with the parameters Δ, $p_{||}$, and $v_{\text{c.m.}}$ According to the theory presented in Sec. V they should depend on the parameters $(p_{||})_{\text{FB}}$ and T_{FB} for the fireball [Eqs. (5.5) and (5.23)]. Figure 6 shows the ratio of the experimental mean parallel momentum of the fragment to the mean momentum $(p_{||})_{\text{FB}}$ of the fireball nucleons as a function of $(p_{||})_{\text{FB}}$. The theoretical values of $(p_{||})_{\text{FB}}$ which we use in this figure are listed in Table I. If we assume that one fireball nucleon gets stuck in the fragment, the ratio $p_{||}/(p_{||})_{\text{FB}}$ should be one. The experimental values show a different behavior: For the 86A MeV systems this ratio is larger than 1 (zone I) and decreases for higher beam energies. It passes the value 1 for beam energies around 500A MeV (zone II) and drops below 1 for higher beam energies (zone III). The physics of this behavior and the meaning of zones I–III will be explained later.

Figure 7 shows the fitted widths Δ of the momentum distribution as a function of the fireball temperature T_{FB}. One recognizes a linear increase (except for the p-Au reaction),

$$\Delta_{\text{fit}} = \Delta_F + \alpha 2mT_{\text{FB}} \tag{6.1}$$

as expected from Eq. (5.5). The straight line represents the theoretical prescription. It is calculated with a Fermi momentum $k_F=240$ MeV/c and assuming that one fireball nucleon gets stuck in the prefragment and deposits all its momentum ($\alpha=1$). The Fermi momentum of 240

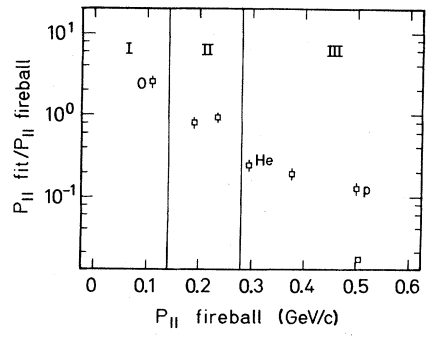

FIG. 6. The mean parallel momentum $p_{||}$ of a fragment $Z=8$ produced in reactions on Au as a function of the mean momentum of one fireball nucleon $(p_{||})_{\text{FB}}$. Each point corresponds to one experiment. The projectile is Ne, except where indicated by a different symbol. The zones I–III refer to different energy regimes and are explained in the caption of Fig. 9.

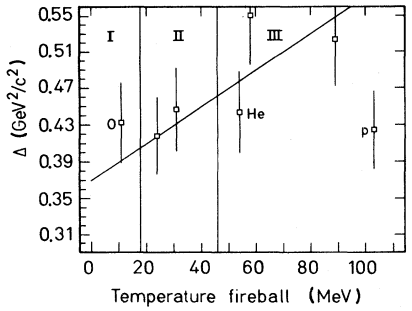

FIG. 7. The width Δ for the fragment momentum distribution for $Z=8$ produced in reactions on Au as a function of the fireball temperature T_{FB}. Note the large offset on the ordinate. The solid line is our prediction. Each point corresponds to one experiment. The projectile is Ne, except where indicated by a different symbol. The zones I–III refer to different energy regimes and are explained in the caption of Fig. 9.

MeV/c corresponds to a slope parameter E_0 in $d\sigma/dE \propto \exp(-E/E_0)$ of

$$E_0=\frac{2}{5}\frac{k^2F}{2M}=12.3 \text{ MeV} . \tag{6.2}$$

One notices a good overall agreement between theory and experiment. However, the discrepancies seem to be systematic. For low beam energies (zone I) the fitted values are slightly higher than the theoretical ones. The agreement is best for zone II, whereas at higher beam energies (zone III) the theory predicts widths which are too large.

Figure 8 displays the velocity $v_{c.m.}$ of the whole system as a function of the dimensionless quantity $(p_{||})_{FB}/T_{FB}$. If $v_{c.m.}$ arises from the viscosity at the interface between fireball and spectator matter as explained in Sec. V, the c.m. velocity should be a linear function of this parameter with a coefficient of proportionality of the order 10^{-3}, Eq. (5.23). One sees a clear correlation between $v_{c.m.}$ and the parameter $(p_{||}/T)_{FB}$. For high beam energies, above 200A MeV (zones II and III), the experimental values follow the predicted linear dependence. For low beam energies (zone I), the experimental values are considerably higher than the predicted ones.

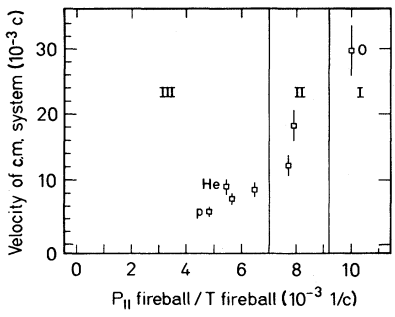

FIG. 8. The center-of-mass velocity $v_{c.m.}$ of the spectator piece as a function of the parameter $(p_{||}/T)_{FB}$ for the fireball. The theory predicts a linear dependence. Each point corresponds to one experiment. The projectile is Ne, except where indicated by a different symbol. The zones I–III refer to different energy regimes and are explained in the caption of Fig. 9.

We conclude as follows: The kinematical parameters Δ, $p_{||}$, and $v_{c.m.}$ which characterize the momentum distribution of the fragments show the behavior which we expect from our picture: The spectator matter bursts into pieces so rapidly that fragments keep the momentum they have had at the moment of breaking. The momentum distribution therefore shows Fermi motion and some momentum which is carried from the fireball into the fragments. While the overall picture seems correct, we observe certain systematic deviations. They seem to be related to the incident energy and may be explained as follows:

One of the assumptions of our model is the complete thermalization of *all* projectile and *all* target participants. It underlies the calculation of T_{FB} and $(p_{||})_{FB}$ as a function of which we have plotted the parameters Δ, $p_{||}$, and $v_{c.m.}$. This assumption is certainly unrealistic in the proton case and depending on the energy also questionable for heavy ion projectiles to some degree. We explain a more realistic situation with the help of Fig. 9.

At low beam energies $E<150A$ MeV (zone I), the projectile is stopped in the target and only part of the geometrically overlapping volumes form a fireball. Therefore, the available energy and momentum are shared by fewer nucleons. This leads to a larger temperature T_{FB} and larger parallel momentum $(p_{||})_{FB}$ per participant. The fireball nucleons cannot escape in the forward direction without moving through the cold spectator matter and accelerating the whole system. For these reasons the velocity $v_{c.m.}$ of the spectator matter is larger than previously calculated. The fitted values of $p_{||}$ and Δ as a function of $(p_{||})_{FB}$ and T_{FB} for 86A MeV agree with our predicted systematics under the assumptions that equilibration takes place between 60% of the geometrically calculated participants.

At energies around 400 MeV (zone II) the standard fireball picture holds. Momentum and energy are shared by all nucleons in the geometrically overlapping zone. Here,

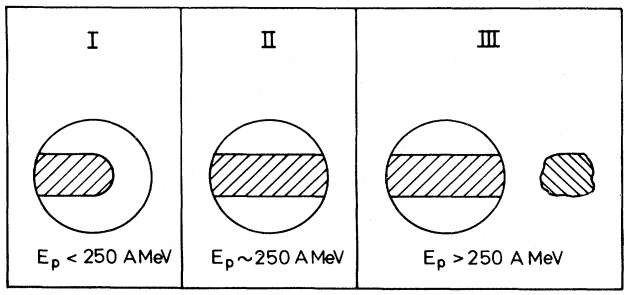

FIG. 9. The three zones in projectile energy and the possible reaction mechanisms: (I) the projectile stops in the target; (II) all geometrically possible participants equilibrate; (III) imperfect equilibration with two fireballs.

TABLE II. The maximal radius R_{max} where a fragment $Z=8$ originates for various reactions. R_{max} is obtained from the Coulomb barriers V_C^{max} according to the procedure described in the text. The theory predicts a value 1 for the values of the last line in the table ($R_T=7.0$ fm, $R_F=3.0$ fm).

Projectile/Target	Ne/Au	Ne/Au	Ne/Au	Ne/Au	He/Au	p/Au	O/Au
Energy (A GeV)	0.25	0.4	1.05	2.1	1.25	4.9	0.084
R_{max}/R_T	0.75	0.74	0.73	0.84	0.74	0.75	0.71
$(R_{max}+R_F)/R_T$	1.8	1.17	1.16	1.27	1.17	1.18	1.14

the fitted values of $v_{c.m.}$, $p_{||}$, and Δ agree with the calculated ones.

At higher energies (zone III) the target participants and the projectile nucleons do not equilibrate completely anymore in one fireball. Two fireballs may be a more appropriate picture. Their temperatures T_{FB} and $(p_{||})_{FB}$ cannot be calculated using energy and momentum conservation alone. The same holds true for the p-A case.

We now turn to the geometrical aspects of the fragmentation reactions. We start with the Coulomb energies. The theoretical distribution $g(V_C)$ [Eq. (5.12)] of Coulomb energies has been derived under the assumptions that the fragments can originate from all possible locations inside the target matter with equal probability. As one sees from the successful fit to the experimental energy and angle distributions (Fig. 3), the distribution function $g(V_C)$ which we have derived describes the broad Coulomb peak well. However, note that the data have an experimental cutoff towards small energies. From the data a maximal Coulomb barrier V_C^{max} is extracted. According to our picture it corresponds to fragments which are emitted from the surface of the nucleus [Eqs. (5.13) and (5.14)]. The values R_{max} can be directly calculated from the experimental values of V_C^{max} via Eq. (5.13). The values for R_{max} which have been determined in this way are shown in Table II and are compared with the target radius R_T and the fragment radius R_F. According to our theory [Eq. (5.14)], the ratio $(R_F+R_{max})/R_T$ should be equal to 1. The experiment is very close to this prediction. The slight deviation may originate in the oblate shape of the prefragments (Fig. 1).

We turn now to the fragment distribution $d\sigma/dZ$. Its shape and absolute value should be given by

$$\frac{d\sigma}{dZ}=\sigma_F\frac{1}{\exp(Z\,1.28/\sqrt{Z_0})-1}\ , \tag{6.3}$$

where Z_0 is the charge of the spectator matter [Eq. (4.10)]. According to Fig. 3 the *shape* of the data is well described by this equation. What about the normalization constant σ_F?

The values obtained by the fit are presented in Table III. They are calculated from the values $d\sigma/dZ$ in Table I and Eq. (6.3). The values of σ_F are of the order of several hundred mb. For a given projectile target combination they do not vary much with energy, but depend strongly on the projectile. Since the total reaction cross sections are of the order of several barns, the fragmentation cross sections σ_F constitute only about 10% of all possible reactions. Fragmentation is considered as a very violent process which corresponds to small impact parameters. If we assume that all collisions with $b<b_{max}$ lead to fragmentation, whereas for larger impact parameters fragmentation does not occur, we can relate σ_F to the impact parameter b_{max} by

$$\sigma_F=\pi b_{max}^2\ .$$

Values of b_{max} are tabulated in Table III for various reactions. For reactions with heavy ions the limit b_{max} seems to correspond to situations where the projectile has completely dived into the target ($b=R_T-R_P$) (see Table III). For He and p as projectiles this geometrical interpretation does not work and the projectile dives in further.

We report another regularity which we have observed but not understood: The experimental values of σ_F seem to depend linearly on the number of participants. However, further data are needed for systematic investigations.

VII. CONCLUSION

We presented an analysis of fragmentation reactions on nuclei induced by high-energy protons or heavy ions. The analysis consists of two parts. First of all, experimental triple differential cross sections $d^3\sigma/d\Omega\,dE\,dZ$ are analyzed for various reactions and the essential physics is extracted and condensed into a few parameters. Any theory of fragmentation reactions should describe the numerical values of all these parameters and their dependence on the specific reaction.

Then we propose a model for the fragmentation reaction which assumes a cold breakup of the spectator

TABLE III. The total fragmentation cross section σ_F for several reactions leading to $Z=8$ fragments. The cross section is converted into a maximal impact parameter b_{max}, which is compared with the situation of complete "dive in" of all projectile nucleons into the target, $b=R_T-R_P$.

Projectile/Target	Ne/Au	Ne/Au	Ne/Au	Ne/Au	He/Au	p/Au	O/Au
Energy (A GeV)	0.25	0.4	1.05	2.1	1.25	4.9	0.084
σ_F (mb)	339	368	547	627	175	73	440
b_{max} (fm)	3.3±1	3.4±0.5	4.2±0.7	4.3±1.1	2.4±0.4	1.5	3.7
R_T-R_P (fm)	3.9	3.9	3.9	3.9	5.1	6.0	4.0

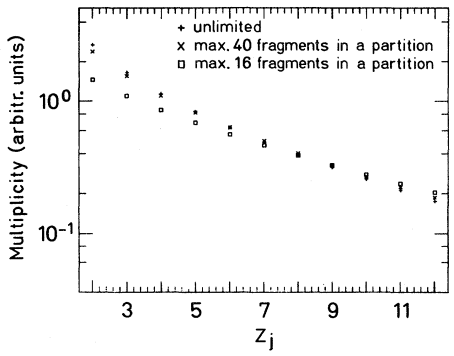

FIG. 10. The multiplicity distributions of fragment charges for various limitations of the total number of fragments.

matter. The word "cold" means the available energy is not equilibrated, rather the spectator matter cracks in a statistical way into several fragments.

The following features of the reaction can be extracted from the data:

(1) Fragmentation reactions are believed to be a violent process. The first well-known indication is a high multiplicity of fast particles (participants) in coincidence with medium mass fragments. We can make the statement more quantitative. In our analysis we are able to extract the total cross section σ_F for fragmentation. When it is related to an impact parameter, we find that the projectile has to dive *completely* into the target nucleus in order to induce multifragmentation.

(2) The target cracks completely. The original location of a prefragment in the spectator piece can be extracted by analyzing the Coulomb peak in the energy distribution. The data indicate that fragments arise from *any* location inside the spectator matter with equal probability. The maximal Coulomb barrier corresponds to fragments from the target surface.

(3) Before cracking, the spectator piece moves with a velocity $v_{\text{c.m.}}$ which is of the order of $1\%c$. Its absolute value as well as its dependence on the incident energy can be understood in the following picture: The projectile drills a hole through the target and the friction or viscosity between participants and the surrounding spectator matter transfers momentum from the projectile to the target spectator.

(4) In the rest system of the spectator matter the fragments have a near isotropic momentum distribution. Its width is compatible with the assumption that it arises from Fermi motion. There is a small dependence of the width on the temperature of the fireball. It agrees with the assumption that one participant nucleon from the fireball carries its momentum into the fragment. This mechanism also explains the deviation of the momentum distribution from isotropy, i.e., it explains the mean momentum in beam direction.

(5) The reaction mechanism seems to depend on the incident energy: For energies below $200A$ MeV the projectile stops in the nucleus. For energies around $500A$ MeV all participants form *one* fireball. Above $1A$ GeV incident energy the participants do not thermalize completely any more and two fireballs seem to be a more appropriate picture.

We have been able to describe *all* data of triple differential cross sections in a consistent and quantitative way. According to our picture the nucleus breaks into pieces in a cold way. One intuitive picture is the shattering of glass. This picture is very appealing. But is the nucleus really brittle? We are rather used to viewing the nucleus as a liquid. We know from macroscopic physics that a droplet of mercury splashes into small droplets under the impact of a force. Is this the more correct analogy for cold breakup of nuclei?

ACKNOWLEDGMENTS

We thank D. Gross and A. Klar for many discussions. W. Müller and I. Bock made a special effort to prepare the data of Ref. 6 for us. One of us (R.I.) would like to thank the Alexander von Humboldt foundation for a fellowship and Prof. H. A. Weidenmüller for his kind hospitality at the Max-Planck-Institut. The work was supported in part by grants from the Gesellschaft für Schwerionenforschung (GSI) and the Bundesministerium für Forschung und Technologie (BMFT).

APPENDIX

A. The inverse Laplace transform of $A(s)$ in the saddle point approximation

In order to determine the parameter s we approximate the inverse Laplace transform of $A(N)$,

$$A(N)=\frac{1}{2\pi i}\int_{-i\infty}^{+i\infty} ds\,\exp\{\ln[A(s)]+sN\} \tag{A1}$$

at the saddle point. The integrand has its maximum for

$$-\frac{d}{ds}\ln[A(s)]=N\ . \tag{A2}$$

Applying this equation to (4.6) one gets

$$N=-\frac{\partial}{\partial s}\sum_i \ln\frac{1}{1-\exp(-si)}=\sum_i \frac{i\exp(-si)m}{1-\exp(-si)}$$

$$=\sum_i \frac{1}{\exp(si)-1}\ . \tag{A3}$$

This sum is converted into an integral

$$N\approx\int_0^\infty di\frac{1}{\exp(si)-1}=\frac{1}{s^2}\zeta(2)\ . \tag{A4}$$

The value of Riemann's zeta function $\zeta(2)$ is 1.644. This leads finally to

$$s=1.28/\sqrt{N}\ . \tag{A5}$$

One can limit the total number of fragments in a partition by introducing step functions into Eqs. (4.1) and (4.2). We do not give details but show the numerical distributions of charge multiplicity for various cases. For $N=65$ Fig. 10 shows the multiplicity for a fragment of size n for three cases: The total multiplicity m is unlimited [Eq. (4.19)] for $m<40$ and $m<16$.

B. Laplace transform of the thermodynamic multiplicity distribution

For the case where the partition function for each fragment is set equal to one, the thermodynamic prediction for $W(s,n)$ is given by

$$W(s,n)=\frac{B(s,n)}{A(s)}$$
$$=\frac{\prod_i \sum_{\{m\}} m_n/m_i!(i!)^{m_i}\exp\left[-s\sum_j m_j j\right]}{\prod_i \sum_{\{m\}} 1/m_i!(i!)^{m_i}\exp\left[-s\sum_j m_j j\right]} . \quad \text{(A6)}$$

Carrying out the summations one arrives at

$$W(s,n)=\frac{\frac{1}{n}\frac{d}{ds}\left\{\sum_{m_n}\exp(-sm_n n)/m_n!/(n!)^{m_n}\right\}}{\sum_{m_n}\exp(-sm_n n)/m_n!/(n!)^{m_n}} , \quad \text{(A7)}$$
$$=\frac{\exp(-sn)}{n!} . \quad \text{(A8)}$$

In order to determine s we again apply the inverse Laplace transform and approximate it by the saddle point method [Eq. (A2)]. Now $A(s)$ has the form

$$A(s)=\sum_{\{m\}}\prod_i \exp\left[-s\sum m_j i\right]/m_i!/(i!)^{m_i} . \quad \text{(A9)}$$

Hence, in the thermodynamic case, N is related to s by

$$\ln N=\exp(-s)-s . \quad \text{(A10)}$$

The dependence (A8) for the fragment distribution fails the experiment completely.

---

*Present address: Cyclotron Laboratory, Department of Physics, Michigan State University, East Lansing, MI 48824.

†On leave from Department of Physics, University of Philippines, Diliman, Quezon City, Philippines.

[1]J. Gosset, H. H. Gutbrod, W. G. Meyer, A. M. Poskanzer, A. Sandoval, R. Stock, and G. D. Westfall, Phys. Rev. C **16**, 629 (1977).

[2]S. Nagamiya, M. C. Lemaire, E. Möller, S. Schnetzer, G. Shapiro, H. Steiner, and I. Taninata, Phys. Rev. C **24**, 971 (1981).

[3]J. Hüfner, K. Schäfer, and B. Schürmann, Phys. Rev. C **12**, 1888 (1975).

[4]L. F. Oliveira, R. Donangelo, and J. O. Rasmussen, Phys. Rev. C **19**, 826 (1979).

[5]A. I. Warwick, H. H. Wiemann, H. H. Gutbrod, M. R. Maier, J. Peter, H. G. Ritter, H. Stelzer, and F. Weik, Phys. Rev. C **27**, 1083 (1983).

[6]I. Bock, U. Lynen, D. Pelte, U. Winkler, R. Glasow, K. H. Kampert, R. Santo, W. F. J. Mueller, A. Gobbi, K. D. Hildenbrand, A. Olmi, H. Sann, and H. Stelzer, Gesellschaft für Schwerionenforschung Scientific Report, 1982, p. 28; I. Bock, Diplomarbeit, Universität Heidelberg, 1983.

[7]J. Randrup and S. E. Koonin, Nucl. Phys. **A356**, 233 (1981); G. Fai and J. Randrup, *ibid.* **A381**, 557 (1982); **A404**, 551 (1983).

[8]D. H. E. Gross, L. Satpathy, Meng Ta-chung, and M. Satpathy, Z. Phys. A **309**, 42 (1982).

[9]G. Bertsch and P. J. Siemens, Phys. Lett. **126B**, 9 (1983).

[10]W. Friedmann and W. Lynch, Phys. Rev. C **28**, 950 (1983).

[11]A. D. Panagiotou, M. W. Curtin, H. Toki, D. K. Scott, and P. J. Siemens, Phys. Rev. Lett. **52**, 496 (1984).

[12]M. A. Cirit and F. Yazici, Phys. Rev. C **23**, 2627 (1981).

[13]S. Bohrmann, J. Hüfner, and M. C. Nemes, Phys. Lett. **120B**, 59 (1983).

[14]L. Winsberg, Nucl. Instrum. Methods **150**, 465 (1978).

[15]A. M. Poskanzer, G. W. Butler, and E. K. Hyde, Phys. Rev. C **3**, 882 (1971).

[16]J. Aichelin and J. Hüfner, Phys. Lett. **136B**, 15 (1984).

[17]I. Dostrovsky, R. Davis, Jr., A. M. Poskanzer, and P. L. Reeder, Phys. Rev. **139**, B1513 (1965).

[18]A. S. Goldhaber, Phys. Lett. **53B**, 306 (1974).

[19]A. Abul-Magd, J. Hüfner, and B. Schürmann, Phys. Lett. **60B**, 327 (1976).

[20]G. D. Westfall, R. G. Sextro, A. M. Poskanzer, A. M. Zebelman, G. W. Butler, and E. K. Hyde, Phys. Rev. C **17**, 1368 (1978).